Langmuir Article

pubs.acs.org/Langmuir

Lyotropic Hexagonal Columnar Liquid Crystals of Large Colloidal Gibbsite Platelets

Maurice C. D. Mourad,* Andrei V. Petukhov, Gert Jan Vroege, and Henk N. W. Lekkerkerker

Van 't Hoff Laboratory for Physical and Colloid Chemistry, Debye Institute for Nanomaterials Science, Utrecht University, The Netherlands

Received February 24, 2010. Revised Manuscript Received July 26, 2010

We report the formation of hexagonal columnar liquid crystal phases in suspensions of large (570 nm diameter), sterically stabilized, colloidal gibbsite platelets in organic solvent. In thin cells these systems display strong iridescence originating from hexagonally arranged columns that are predominantly aligned perpendicularly to the cell walls. Small angle X-ray scattering and polarization microscopy indicate the presence of orientational fluctuations in the hexagonal columnar liquid crystal phase. The presence of decoupling of the average platelet orientation and the column axis as well as column undulations leading to a decrease of the effective column diameter are discussed. The fact that these phenomena are particularly pronounced in the vertical direction and are enhanced toward the bottom part of the system points to the role of gravitational compaction on the structure.

Introduction

In many respects colloidal particles behave very similar to atoms and molecules and display intriguing phase transitions between gas, liquid, solid and a rich variety of liquid crystalline phases.[1−4] Colloidal particles with nonspherical shapes (such as rods and plates) are of particular interest because of their ability to form liquid crystals. Nematic liquid crystals possess orientational order; smectic and columnar liquid crystals additionally exhibit positional order (in one and two dimensions respectively). The phase separation in suspensions of anisometric colloidal particles into an isotropic and a nematic phase was addressed theoretically by Onsager[6] in the 1940s. He demonstrated that the thermodynamic stability of the nematic phase can be explained on a purely entropic basis by considering the competition between orientational entropy (favoring the isotropic state) and the entropy of the excluded volume (which favors the nematic state). As the latter becomes more important at higher concentrations, a first-order transition from an isotropic to a nematic phase may occur if the concentration of rods or plates is sufficiently high. Thus, even hard rods or plates may form a nematic phase. Evidence that a system of hard rods can form a thermodynamically stable smectic phase[7] and a system of hard platelets can form a thermodynamically stable columnar phase[8] was provided by computer simulations in the 1980s and 1990s. While liquid crystal phase transitions in suspensions of rod-like particles have been observed for a long time it is only in the last ten years that firm experimental evidence for liquid crystal phase equilibria in suspensions of plate-like particles was obtained.[9−17]

The liquid crystal phase behavior of suspensions of small colloidal gibbsite platelets has been explored extensively.[3,10,11,18,19] These particles of approximately 150−200 nm in diameter can be synthesized conveniently by hydrothermal treatment of alumina alkoxides in acidic solution.[25] Suspensions of both sterically and charge stabilized gibbsite platelets synthesized in this way do display nematic and columnar phases upon increasing the concentration. Because of the intercolumnar periodicity, the columnar phases of these colloidal gibbsite platelets exhibit strong Bragg reflections in the visible range.[11,18,19] Moreover, they have been used as templates for the generation of ordered silica structures.[20]

In the present work the spontaneous formation of the columnar structure by larger gibbsite platelets is investigated. First of all, our aim is to make use of larger platelets in order to make them observable in microscopy and be able to study the periodic columnar structure and its defects in real space. Second, increasing the period of the self-assembled structure may allow for novel applications such as photonics.[5] Larger gibbsite particles can be grown using a seeded growth procedure.[21] Alternatively, large particles can be synthesized by coprecipitation of aluminum nitrates[22] and subsequent

*To whom correspondence should be addressed. E-mail: m.mourad@ucl.ac.uk.

(1) Pusey, P. N.; van Megen, W. *Nature* **1986**, *320*, 340–342.
(2) Anderson, V. J.; Lekkerkerker, H. N. W. *Nature* **2002**, *416*, 811–815.
(3) Mourad, M. C. D.; Byelov, D. V.; Petukhov, A. V.; de Winter, D. A. M.; Verkleij, A. J.; Lekkerkerker, H. N. W. *J. Phys. Chem. B* **2009**, *113*, 11604–11613.
(4) van den Pol, E.; Petukhov, A. V.; Thies-Weesie, D. M. E.; Byelov, D. V.; Vroege, G. J. *Phys. Rev. Lett.* **2009**, *103*, 258301.
(5) Wijnhoven, J. E. G. J.; Vos, W. L. *Science* **1998**, *281*, 802–804.
(6) Onsager, L. *Ann. N.Y. Acad. Sci.* **1949**, *51*, 627–659.
(7) Frenkel, D.; Lekkerkerker, H. N. W.; Stroobants, A. *Nature* **1988**, *332*, 822–823.
(8) Veerman, J. A. C.; Frenkel, D. *Phys. Rev. A* **1992**, *45*, 5632–5648.
(9) Brown, A. B. D.; Clarke, S. M.; Rennie, A. R. *Langmuir* **1998**, *14*, 3129–3132.
(10) van der Kooij, F. M.; Lekkerkerker, H. N. W. *J. Phys. Chem. B* **1998**, *102*, 7829–7832.
(11) van der Kooij, F. M.; Kassapidou, K.; Lekkerkerker, H. N. W. *Nature* **2000**, *406*, 868–871.
(12) Liu, S.; Zhang, J.; Wang, N.; Liu, W.; Zhang, C.; Sun, D. *Chem. Mater.* **2003**, *15*, 3240–3241.
(13) van der Beek, D.; Lekkerkerker, H. N. W. *Europhys. Lett.* **2003**, *61*, 702–707.
(14) van der Beek, D.; Lekkerkerker, H. N. W. *Langmuir* **2004**, *20*, 8582–8586.
(15) Fossum, J. O.; Gudding, E.; Fonseca, D. D. M.; Meheust, Y.; DiMasi, E.; Gog, T.; Venkataraman, C. *Energy* **2005**, *30*, 873.
(16) Michot, L. J.; Bihannic, I.; Maddi, S.; Funari, S. S.; Baravian, C.; Levitz, P.; Davidson, P. *Proc. Natl. Acad. Sci. U.S.A.* **2006**, *103*, 16101–16104.
(17) Sun, D.; Sue, H.-J.; Cheng, Z.; Martínez-Ratón, Y.; Velasco, E. *Phys. Rev. E* **2009**, *80*, 041704.
(18) van der Kooij, F. M.; van der Beek, D.; Lekkerkerker, H. N. W. *J. Phys. Chem. B* **2001**, *105*, 1696–1700.
(19) van der Beek, D.; Petukhov, A. V.; Oversteegen, S. M.; Vroege, G. J.; Lekkerkerker, H. N. W. *Eur. Phys. J. E* **2005**, *16*, 253–258.
(20) Mourad, M. C. D.; Groeneveld, E.; de Lange, P. J.; Vonk, C.; van der Beek, D.; Lekkerkerker, H. N. W. *J. Mater. Chem.* **2008**, *18*, 3004–3010.
(21) Wijnhoven, J. E. G. J. *J. Colloid Interface Sci.* **2005**, *292*, 403.
(22) Shen, S.; Chow, P. S.; Chen, F.; Feng, S.; Tan, R. B. H. *J. Cryst. Growth* **2006**, *292*, 136.

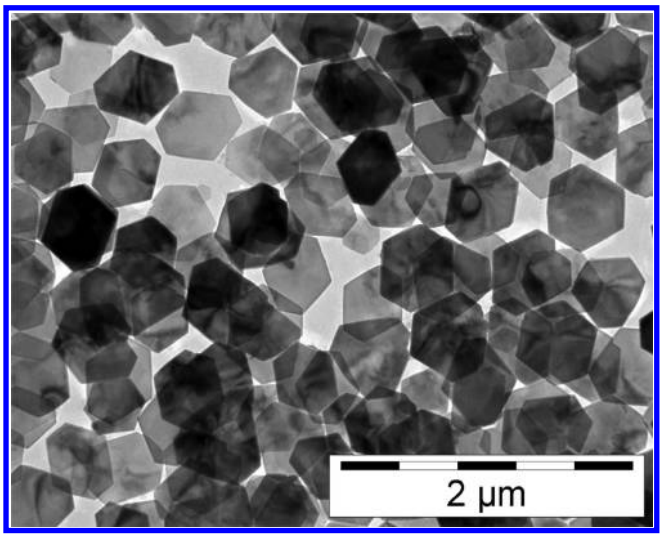

Figure 1. Transmission electron micrograph of the sterically stabilized gibbsite platelets.

hydrothermal treatment. However, the effect of gravity quickly enhances as a fourth power as a result of upscaling of the particle dimensions.

Wijnhoven et al. observed that large gibbsite platelets with an average diameter of 570 nm in water upon sedimentation formed glassy sediments rather than columnar crystals.[23] Recently, Houghton and Donald provided detailed insight in these structures using environmental scanning electron microscopy.[24] While these platelets were at the size threshold of what can be distinguished in optical microscopy their liquid crystal behavior seemed to be severely impaired as a result of the increased effect of sedimentation.

In this paper, we demonstrate that sterical stabilization with polyisobutylene chains enables same large (570 nm) gibbsite particles to form beautiful hexagonal columnar phases in tetralin. In thin cells (thickness ~0.15 mm) these columnar phases are formed in a matter of hours. The appearance of iridescence colors suggests that the columns are uniformly ordered over centimeters and oriented in average perpendicularly to the glass walls of the sample cell. Despite their appearance and quick formation, detailed high resolution small angle X-ray scattering (SAXS) measurements indicate the considerable influence of gravity on the structure. In particular, we observe decoupling between the column axes and the particle orientation, which is particularly pronounced near the bottom of the sample and is stronger in the vertical direction. As a result, the average column diameter appears somewhat smaller than the particle diameter. The decoupling can be interpreted as an effect of undulations in the columns and by tilting of the particles within columns due to a gravity-induced uniaxial mechanical stress in the vertical direction. The results exemplify that one has to remain observant of side effects while scaling-up particle sizes in colloidal liquid crystals.

Experimental Section

Synthesis. Colloidal, hexagonal gibbsite platelets were prepared in a seeded growth experiment and characterized by Wijnhoven.[21] The platelet thickness and length (D) are measured to be 47 nm (±23%) and 570 nm (±11%) by atomicforce microscopy (AFM) and transmission electron microscopy (TEM, Figure 1), respectively. The particle surfaces were grafted by amino modified poly isobutylene chains (SAP230TP, Infineum U.K. Ltd.) following a novel approach developed by us.[26] For this purpose aqueous gibbsite particles are mixed with an excessive amount of SAP230TP (1.5 g/g particles) dispersed in *n*-propanol (Acros, 99%). Subsequently the solvent is removed in a two-step process. First a substantial part of the water and *n*-propanol is extracted using a rotary evaporator, while the temperature is raised to 40 °C. Then the remaining solvent is extracted by freezing the sample by immersion of the flask in liquid nitrogen followed by connection to a vacuum setup for freeze-drying. The sample is redispersed in toluene (J. T. Baker, 99.5%). Finally the excess of SAP230TP is removed by centrifugation of the particles followed by redispersion in toluene (repeated two times). This way allows batches of polymer grafted inorganic particles to be produced with relative ease. The dispersion is centrifuged and redispersed twice in tetralin (1,2,3,4-tetrahydronaphtalene, Acros 98%).

Sample Preparation. Dilute suspensions of the sterically stabilized gibbsite particles were concentrated by moderate centrifugation (30 min, <200g) and subsequent removal of the supernatant, followed by redispersion. The concentrated suspensions with an estimated solid content of 50% wt thus obtained were put in sample cells (inner cross section approximately 15 × 0.15 mm and height 15 mm) made of two flat glass plates (G. Menzel, Glasbearbeitungswerk GmbH, Germany, thickness 0.13−0.16 mm). The shorter sides of the cells consisted of two-component tetralin-insoluble epoxy resin (Araldit AW2101, Vantico AG, Switzerland) and were suitable for both optical and X-ray scattering experiments due to their small optical path length and limited glass wall thickness.

Polarization Microscopy. The liquid crystalline sample was studied using a Nikon polarization microscope (Eclipse LV100pol) equipped with a digital camera (QImaging, MP5). The optical birefringence was determined with the help of retardation filters (optical path difference 530 nm), inserted at an angle of 45° with respect to both the polarizer and analyzer.

Laser Diffraction. In order to study the periodicity in the liquid crystalline suspension laser diffraction experiments were performed using a variable wavelength Krypton-ion laser (Spectra Physics, 2025−11) operated at 47.6A producing 0.11 W 476.5 nm wavelength light. The sample cell was mounted in the middle of a partly sandblasted round-bottom flask that was filled with toluene. In this way, reflections at the surface of the sample cell -which was oriented at an angle of 45 deg with respect to the incoming laser beam- could be minimized (see also ref 27). The flask was equipped with an entrance window for the laser beam. We can calculate the scattering angle θ (defined as the angle between the direct and the scattered beam) for the Bragg peaks by measurement of the distance between the direct and the diffracted laser beams over the surface of the flask taking the diameter of the flask into account. The d-spacings responsible for these diffractions can be calculated as follows:

$$d = \frac{\lambda}{2n_s \sin\left(\frac{\theta}{2}\right)} \quad (1)$$

where λ is the wavelength of the laser *in vacuo*, n_s is the index of refraction of the solvent, and θ is the scattering angle.

Small Angle X-ray Scattering (SAXS). Experiments were performed at the SAXS/WAXS station of the DUBBLE beamline BM-26B[28] at the ESRF (Grenoble, France) using a microradian

(23) Wijnhoven, J. E. G. J.; van 't Zand, D. D.; van der Beek, D.; Lekkerkerker, H. N. W. *Langmuir* **2005**, *21*, 10422–10427.
(24) Houghton, H. A.; Donald, A. M. *Scanning* **2008**, *30*, 223–227.
(25) Wierenga, A. M.; Lenstra, T. A. J.; Philipse, A. P. *Colloids Surf., A* **1998**, *134*, 359–371.
(26) Mourad, M. C. D.; Devid, E. J.; van Schooneveld, M. M.; Vonk, C.; Lekkerkerker, H. N. W. *J. Phys. Chem. B* **2008**, *112*, 10142–10152.
(27) Sanders, J. *Acta Crystallogr. A* **1968**, *24*, 427–434.
(28) Borsboom, M.; Bras, W.; Cerjak, I.; Detollenaere, D.; van Loon, D. G.; Goedtkindt, P.; Konijnenburg, M.; Lassing, P.; Levine, Y. K.; Munneke, B.; Oversluizen, M.; van Tol, R.; Vlieg, E. *J. Synchrotron Radiat.* **1998**, *5*, 518–520.

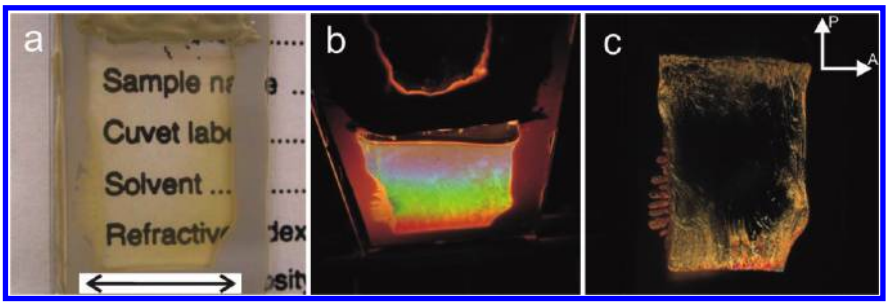

Figure 2. (a) Demostration of the translucent properties of the sample. The arrow denotes 17 mm, which corresponds to the width of the cell. (b) Cell illuminated by a white light source. The variation of the colors is related to the variation in the viewing angle. (c)Sample in between crossed polarizers (indicated in the upper right corner by *P* and *A*, respectively).

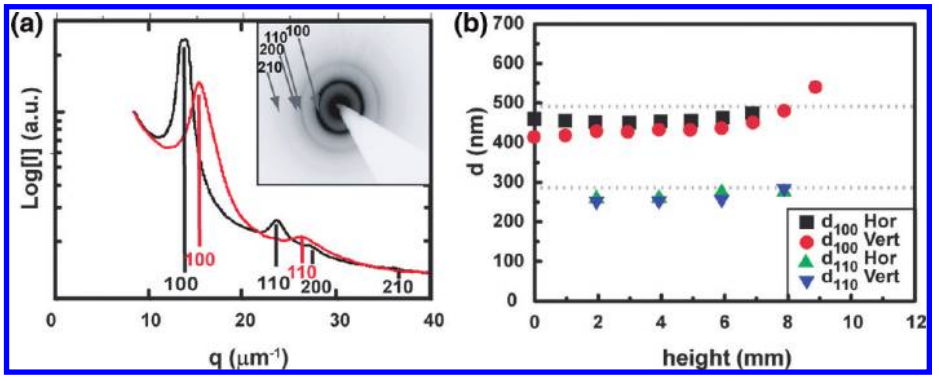

Figure 3. (a) Profiles of the X-ray scattering intensity in the horizontal (black curve) and vertical (red curve) direction. The inset shows the 2D high resolution SAXS pattern. (b) d_{100} and d_{110} recorded in the horizontal (Hor) and vertical (Vert) direction at different heights above the bottom of the sample. The dashed lines indicate the d_{100}^{ideal} and d_{110}^{ideal}, assuming an intercolumnar distance equal to the diameter of the platelets (570 nm).

setup similar to the one described earlier.[29] A monochromatic 15 keV X-ray beam (wavelength $\lambda = 0.83$ Å, spectral width $\Delta\lambda/\lambda = 2 \times 10^{-4}$) was selected using a Si-111 monochromator and focused on the detector by a set of compound refractive lenses.[30] The sample was at 8 m distance from the X-ray sensitive CCD detector (VHR, Photonics Science, 4008 × 2671). The sample cell was mounted on a remotely controlled, motorized translation stage. Measurements were taken typically with steps of 1 mm along both the vertical and horizontal direction through the middle part of the sample cell. Scattering patterns were corrected for a background signal, taking into account the absorption by the sample.

Results and Discussion

Directly after dispersion in tetralin the colloidal suspension of gibbsite platelets had a pale green color. The turbidity is remarkably low, despite the high concentration and the large platelet diameter. This is illustrated in Figure 2a, where it is shown that the dispersion is transparent. Within hours after transfer of the dispersion into the sample cell the colloidal suspension became iridescent and displayed bright Bragg reflections ranging from violet to red upon increase of the scattering angle (Figure 2b). The middle of the sample cell appeared relatively dark in crossed polarizers. In contrast, the sides of the sample cell displayed strong birefringence (Figure 2c). Apparently, in the middle part there is homeotropic anchoring of the platelets to the glass substrate (platelet surface parallel to the substrate). In this particle orientation the two identical indices of refraction of the uniaxial mineral are both situated in the optical plane while the second index of refraction is oriented perpendicular to the walls. This leads to absence of birefringence in the optical configuration employed. This observation is confirmed by the fact that tilting the glass cell around a vertical rotation axis such that the glass walls are not oriented parallel to the polarizers anymore made the cell appear birefringent, as the second index of refraction of the mineral then entered the optical plane. At the sides of the sample cell birefringence is observed. This we ascribe to the perturbing effect of the side walls on the orientation of the platelets.

As the dispersion is strongly iridescent the structure of the dispersion could be studied conveniently by laser light diffraction, which was performed 3 days after preparation. On the round-bottom flask that was used as a projection screen as described above three Bragg peaks could be discerned visually. The positions of the diffraction peaks in the horizontal plane are estimated to be at scattering angles of approximately 37.8°, 67.6° and 76.4°. Assuming 1.54 for n_s, this would lead to *d*-values of 478 nm, 278 and 250 nm. The ratio of the corresponding *q*-values (1:1.71:1.91) is in reasonable agreement with the ratio ($1:3^{1/2}:4^{1/2}$) indicative of the q_{100}, q_{110}, and q_{200} in a hexagonal lattice. This we ascribe to the formation of a hexagonal columnar liquid crystal.

A more detailed picture was obtained by small-angle X-ray diffraction. Typical X-ray scattering intensity profiles and a 2D X-ray scattering pattern obtained 5 months after preparation of the iridescent sample are displayed in Figure 3a.

At low *q*-values up to four concentric Bragg reflections were observed. Interestingly, these reflections are elliptical rather than round and display elongations that are similar for all reflections. The ratios of the corresponding *q*-values were in agreement with the characteristic ratios of $1:3^{1/2}:4^{1/2}:7^{1/2}$ of the hexagonal lattice. The 100 peaks are well-defined and their position could be determined much more accurately than in the laser diffraction

(29) Petukhov, A. V.; Thijssen, J. H. J.; 't Hart, D. C.; Imhof, A.; van Blaaderen, A.; Dolbnya, I. P.; Snigirev, A.; Moussaid, A.; Snigireva, I. *J. Appl. Crystallogr.* **2006**, *39*, 137–144.
(30) Snigirev, A.; Kohn, V.; Snigireva, I.; Lengeler, B. *Nature* **1996**, *384*, 49.

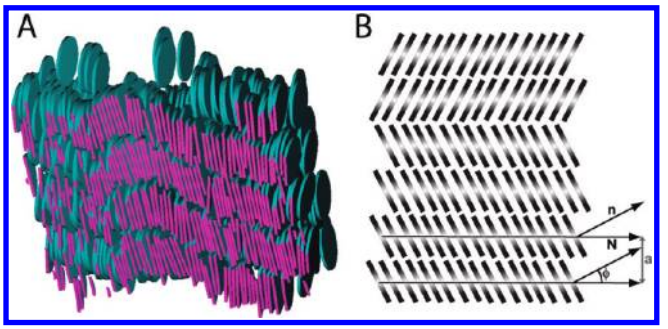

Figure 4. Two mechanisms of decoupling of the platelet normal and the column axis. (A) Intersection of a snapshot from a hexagonal columnar phase in computer simulations on hard disks, kindly provided by Tanja Schilling (c = 8.66, Π = 82.5),[31] that illustrates the presence of significant column undulations. The broadening of the diffraction spots originating from such a system can give rise to a shift of the Bragg peak in X-ray scattering experiments to larger q-values. (B) Cartoon of a hexagonal columnar phase is depicted in which the column orientation **N** makes an angle ϕ with the average particle director $\langle \mathbf{n_i} \rangle$, such that ultimately the intercolumnar spacing **a** can become smaller than the particle diameter.

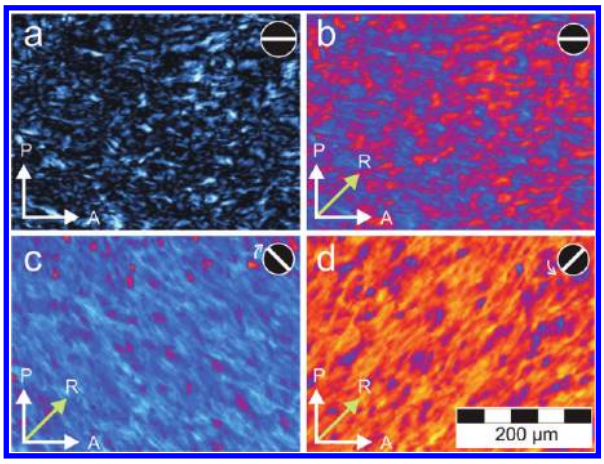

Figure 5. Polarized light micrographs of the system without (a) and with (b, c, d) retardation plate of 530 nm. The orientation of the polarizer and analyzer are indicated by P and A, respectively, while the slow axis of the retardation filter is indicated as R. In the upper right corner the horizontal direction is indicated: the cell was tilted by 45° clockwise (c) and counter-clockwise (d), giving rise to different interference colors.

experiments (within 1%). Higher order peaks, in particular 200, are not as well-defined and, in some cases, could not be observed in the scattering patterns.

At higher q, a liquid-like Bragg peak for the (intracolumnar) 001 reflection is visible in scattering patterns of some locations within the sample cell. Presumably, this observation is due to the presence of domains with orientations other than the ones with columns perpendicular to the cell walls that were described earlier. The correlation distances for these 001 reflections corresponded typically to around 70 nm with a full width of the peak that was about 20% of the q_{001} value. Otherwise, the 001 reflection is not observed. Scattering patterns, obtained by rotation of the sample cell in the X-ray beam, as well as a scattering pattern in which the 001 reflection is visible are provided as Supporting Information. They confirm the preferential column orientation along the cell normal due to particle anchoring at the flat walls. Upon going from the top toward the bottom of the sample the q-values of the intercolumnar reflections slightly increase indicating compaction of the structure (see Figure 3*b* in which all observable 100 and 110 peaks along the horizontal and vertical direction are included). Furthermore, the low q reflections become increasingly elliptical. This is surprising as the gravitational length of the gibbsite platelets ($l_g = k_BT/(\Delta m g)$ = 30 μm, where k_BT is the thermal energy, Δm is the buoyant mass of the particles in the solvent and g is the gravitational acceleration) is much larger than the period of the structure and hence no direct influence of the gravity on the structure can be expected. Even more surprisingly, the d-values $d_{hkl} = 2\pi/q_{hkl}$ calculated from the Bragg peak positions appear to be smaller than those expected for an ideal hexagonal columnar structure with the intercolumnar distances based on the average particle diameter D: $d_{100}^{\text{ideal}} = 3^{1/2}D/2$ and $d_{110}^{\text{ideal}} = D/2$. To rationalize these surprising results, we have assumed that the normal to the particles $\mathbf{n}_i$ and the column axes **N** can deviate from each other. There could be different reasons for such decoupling. For example, fluctuations of the structure might lead to particles sliding over each other, as in the simulation result shown in Figure 4A. Here one can see that while the particles remain parallel to each other, the column direction **N** can significantly deviate from the average particle normal $\langle \mathbf{n}_i \rangle$ in (part of) the column.

(31) van der Beek, D.; Schilling, T.; Lekkerkerker, H. N. W. *J. Chem. Phys.* **2004**, *121*, 5423–5426.

We also note that the effect is seen to be much stronger in the vertical direction, which points toward the direct role of gravity. A uniaxial stress of the columnar structure in the vertical direction can also cause decoupling between $\langle \mathbf{n}_i \rangle$ and **N** without the need for a deformation of the column itself. In Figure 4B, the platelets can then be tilted within their columns. As illustrated in the figure, the effective (local) size of each column can in both cases be reduced to $D \cos \phi$, where D is the platelet diameter and ϕ is the angle between $\langle \mathbf{n}_i \rangle$ and **N**. This reduction of the effective column size can reduce the average intercolumnar distance and, therefore, can shift the diffraction peaks to slightly larger q-values.

SAXS measurements were carried out again 10 months after preparation of the sample. The results of this experiment closely resemble the results of the first set of measurements. This suggests the long-term stability of the proposed structures.

Furthermore, measurements were performed at various degrees of rotation of the sample cell within the X-ray beam (see Supporting Information). Rotation by angles up to 60° does not lead to significant changes in the position of the intercolumnar Bragg reflections. In the horizontal scattering plane, however, the relative intensity of the latter are slowly reduced. The relative position and the relative intensity of the intercolumnar reflections are not affected by changes in the sample absorption or the scattering volume as a result of the rotation.

As can be seen from Figure 3a the intensity of the intercolumnar 100 and 110 reflections is somewhat weaker in the vertical direction than in the horizontal direction. This can be understood as an effect of column undulations such as illustrated in Figure 4A. Significant fluctuations of the orientations of the columnar network may be present, which would be congruent to the column undulation mechanism sketched in Figure 4A. We note that fluctuation effects of these types are not necessarily limited to colloidal platelets.

Support for the hypothesis that orientational fluctuations are stronger in the vertical than in the horizontal direction comes from polarization microscopy. In this technique the average particle orientation ($\langle \mathbf{n}_i \rangle$) rather than the column direction (**N**) is measured. For colloidal gibbsite platelets it has been shown in a system in which the platelets were oriented at the isotropic−nematic interface that a larger component of the index of refraction is oriented

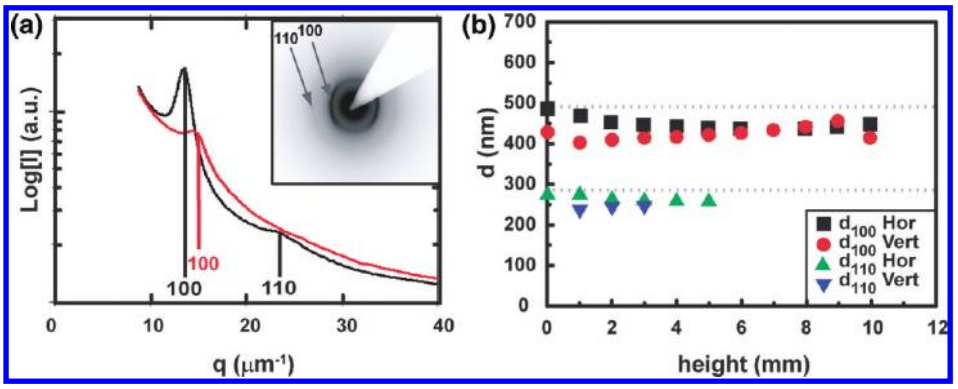

Figure 6. (a) Profiles of the X-ray scattering intensity in the horizontal (black curve) and vertical (red curve) direction of the concentrated sample. The inset shows the 2D high resolution SAXS pattern. (b) d_{100} and d_{110} recorded in the horizontal (Hor) and vertical (Vert) direction at different heights above the bottom of the sample.The dashed lines indicate the d_{100}^{ideal} and d_{110}^{ideal} assuming an intercolumnar distance based on the average diameter of the platelets (570 nm) and an ideal hexagonal lattice.

normal to the platelet surface than in the plane of this surface.[34] This holds in particular for suspensions in which the contribution of the birefringence due to the shape of these particles is negligible due to a small difference in the index of refractions of the particles and the dispersion medium (toluene, tetralin). As a result, any projection of the platelet normal that is not parallel to the optical axis of the microscope or one of the polarizing filters will contribute to birefringence. In practice, all these contributions will equal out unless there is a preferred orientation of the particles along the optical axis. In polarization microscopy, the optical path difference (OPD) of transmitted polarized light can be determined.[32] Insertion of a retardation filter (λ-plate, a birefringent crystal), oriented at 45° with respect to the polarizer and analyzer, changes the offset of the OPD. When the orientation of the particle director is parallel to the slow axis of a retardation filter the OPD of the particles will be cumulative to the OPD of the retardation filter, leading to a large observable OPD. In contrast, when the orientation of the particle director is perpendicular to the slow axis of the retardation filter the OPD of particles will be subtracted from the OPD of the retardation filter leading to a smaller observable OPD. By this effect the polarization micrographs that are taken with a retardation filter indicate the preferred orientation of the platelets in different domains of the sample. In Figure 5 polarization micrographs of the columnar crystal with and without retardation filter are displayed. It appears that there is a considerable part of the sample in which the orientation of the particles averaged over the thickness of the sample cell have a preferential orientation that is not perpendicular to the glass wall (blueish-white areas in Figure 5a). Insertion of the retardation filter (Figure 5b) reveals which of these areas have particle orientations that are parallel to the slow axis of the filter (blue domains) and perpendicular to this axis (orange domains). Confirmation that the orientational fluctuations are predominantly present in the vertical direction of the sample is obtained by rotation 45° of the sample within the optical plane in the microscope (Figure 5, parts c and d). Higher interference colors (light blue) severely dominate in case the vertical direction in the sample coincides with the slow axis of the retardation filter (Figure 5c). In contrast, lower interference colors (yellow) dominate in case the vertical direction in the sample is oriented perpendicularly to this axis (Figure 5d). Hence the interference color patterns

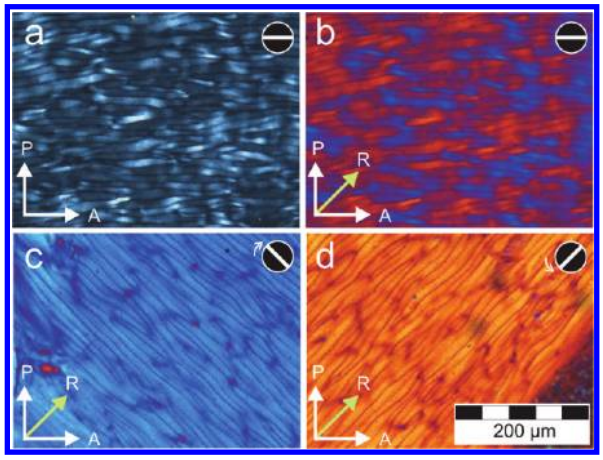

Figure 7. Polarized light micrographs of the concentrated system without (a) and with (b, c, d) retardation plate of 530 nm. The orientation of the polarizer and analyzer are indicated by *P* and *A*, respectively, while the slow axis of the retardation filter is indicated as *R*. In the upper right corner the horizontal direction is indicated: the cell was tilted by 45° clockwise (c) and counter-clockwise (d) giving rise to different interference colors.

clearly support a preferential orientation of the slow axis of the index of refraction and thus of **n** in the vertical direction rather than in the horizontal direction, similar as depicted in Figure 4B.

In one of the samples, the columnar phase was concentrated further by very slow evaporation of the solvent (remaining still liquid after a period of more than 2 years). This dispersion displayed a higher turbidity and stronger birefringence than the original, but did not lose its striking iridescence.

SAXS experiments were performed on this 2.5 year old, concentrated sample (Figure 6). The long-range hexagonal order appeared to be decreased. The 100, 110, and 001 were the only Bragg peaks left to be observed and appeared to have broadened over time. Again, the intercolumnar 100 and 110 reflections is somewhat weaker in the vertical direction than in the horizontal direction. Furthermore, these experiments indicate a similar difference in q-values between the scattering in the horizontal and vertical direction as described before (see Figure 6b in which all observable 100 and 110 peaks along the horizontal and vertical direction are included). Evaporation of the solvent can affect the liquid crystalline order via an increase of the osmotic pressure, which enhances polydispersity-induced structure frustration.[35]

(32) Robinson, P. C. B., *Qualitative Polarized Light Microscopy*; Oxford University Press-Royal Microscopical Society: Oxford, U.K., 1992; Chapter 2
(33) Maeda, H.; Maeda, Y. *Langmuir* **1996**, *12*, 1446–1452.
(34) van der Beek, D.; Reich, H.; van der Schoot, P. P. A. M.; Dijkstra, M.; Schilling, T.; Vink, R.; Schmidt, M.; van Roij, R.; Lekkerkerker, H. N. W. *Phys. Rev. Lett.* **2006**, *97*, 087801.
(35) Petukhov, A. V.; van der Beek, D.; Dullens, R. P. A.; Dolbnya, I. P.; Vroege, G. J.; Lekkerkerker, H. N. W. *Phys. Rev. Lett.* **2005**, *95*, 077801.

Moreover, much stronger structure compression is induced by capillary forces at the final stage of the drying.[36]

The textures that are observable in polarization microscopy have significantly evolved after the slow evaporation of solvent. Rather than granular patterns, periodic textures that may be related to column undulations are visible (Figure 7). These textures show broad similarities to earlier published patterns of columnar phases of colloidal rods.[37,38] The undulating patterns have a periodicity of about 10 μm in the vertical direction and 50 μm in the horizontal direction. The retardation colors in Figure 7, parts a and b, compared to those in Figure 7, parts c and d, clearly indicate that the particle director still deviates preferentially in the vertical direction and has additionally some components along the horizontal direction as described above. Furthermore, rotation of the sample with respect to the polarizers indicates that the dark lines that mark the periodic textures correspond to boundary regions in which the platelets are oriented parallel to the glass walls of the sample cell. We note that despite extensive studies, oval-shaped Bragg peaks were never observed in X-ray scattering experiments for liquid crystals of gibbsite platelets with a smaller diameter (of about 200 nm). Our results illustrate that scaling-up the particle size may lead to side effects which need to be carefully considered. It is clear that the role of gravity has drastically increased in the system studied here. In particular, we find decoupling between the particle orientation and the column orientations, which can proceed via fluctuations of the column directions keeping the particle orientation unchanged (Figure 4A) and via fluctuations of the particle orientations keeping the column orientation unaffected (Figure 4B). Our results suggest that both mechanisms are present in the systems studied. We also note that fluctuation effects of these types are not necessarily limited to colloidal platelets. For example, considerable variation of the particle orientations and layer undulations have been observed in the lyotropic smectic phase of colloidal β-FeOOH rods in scanning electron microscopy images[33] and recently in X-ray scattering experiments on α-FeOOH boards.[39]

(36) Petukhov, A. V.; Dolbnya, I. P.; Aarts, D. G. A. L.; Vroege, G. J. *Phys. Rev. E* **2004**, *69*, 031405.
(37) Livolant, F.; Bouligand, Y. *J. Phys.* (*Paris*) **1986**, *47*, 1813–1827.
(38) Grelet, E. *Phys. Rev. Lett.* **2008**, *100*, 168301.
(39) van den Pol, E. *Goethite liquid crystals and magnetic field effects*. Ph.D. Thesis, Utrecht University: Utrecht, The Netherlands, 2010.

Conclusions

Concentrated suspensions of large sterically stabilized gibbsite particles form hexagonal columnar phases in flat sample cells in a matter of hours. Iridescence and polarization microscopy indicate a rather uniformly ordered structure in which columns are predominantly oriented perpendicular to the glass walls of the sample cell. SAXS and polarization microscopy amend this view on the structures formed and clearly indicate the presence of orientational fluctuations in the form of particle director orientation fluctuations and column undulations. Furthermore, the difference of these fluctuations in the vertical direction direction compared to the horizontal direction imply the strong effect of gravitational compaction in the structure. These phenomena are particularly pronounced in the columnar phase of large platelets.

Acknowledgment. B. W. M. Kuipers is kindly acknowledged for assistance in the laser diffraction measurements. J. E. G. J. Wijnhoven is thanked for providing the aqueous gibbsite sample and T. Schilling is thanked for sharing the simulation data. J. H. J. Thijssen and A. A. Verhoeff are thanked for discussions and critical reading of the manuscript. J. D. Meeldijk and the Electron Microscopy Group (Utrecht University) are thanked for their TEM support. A. Snigirev and the personnel of the DUBBLE beamline at ESRF, Grenoble are acknowledged for their excellent support. Infineum U.K. Ltd. is acknowledged for donation of the SAP 230TP. The Netherlands Organization for Scientific Research (NWO) is thanked for financial support of MCDM and the beam time provided.

Supporting Information Available: Figures showing scattering patterns, obtained by rotation of the sample cell in the X-ray beam, as well as a scattering pattern in which the 001 reflection is visible and text discussing the figures. This material is available free of charge via the Internet at http://pubs.acs.org.